Physics Letters B 821 (2021) 136613

Contents lists available at ScienceDirect

Physics Letters B

www.elsevier.com/locate/physletb

Longitudinal **Z**-boson polarization and the Higgs boson production cross section at the Large Hadron Collider

S. Amoroso [a], J. Fiaschi [b,c], F. Giuli [d,e], A. Glazov [a], F. Hautmann [f,g,*], O. Zenaiev [d]

[a] *Deutsches Elektronen-Synchrotron DESY, D 22607 Hamburg, Germany*
[b] *Department of Mathematical Sciences, University of Liverpool, Liverpool L69 3BX, United Kingdom of Great Britain and Northern Ireland*
[c] *Institut für Theoretische Physik, Universität Münster, D 48149 Münster, Germany*
[d] *CERN, CH-1211 Geneva 23, Switzerland*
[e] *University of Rome Tor Vergata and INFN, Sezione di Roma 2, 00133 Roma, Italy*
[f] *Elementaire Deeltjes Fysica, Universiteit Antwerpen, B 2020 Antwerpen, Belgium*
[g] *Theoretical Physics Department, University of Oxford, Oxford OX1 3PU, United Kingdom of Great Britain and Northern Ireland*

A R T I C L E   I N F O

Article history:
Received 11 May 2021
Received in revised form 11 August 2021
Accepted 30 August 2021
Available online 6 September 2021
Editor: A. Ringwald

A B S T R A C T

Charged lepton pairs are produced copiously in high-energy hadron collisions via electroweak gauge boson exchange, and are one of the most precisely measured final states in proton-proton collisions at the Large Hadron Collider (LHC). We propose that measurements of lepton angular distributions can be used to improve the accuracy of theoretical predictions for Higgs boson production cross sections at the LHC. To this end, we exploit the sensitivity of the lepton angular coefficient associated with the longitudinal Z-boson polarization to the parton density function (PDF) for gluons resolved from the incoming protons, in order to constrain the Higgs boson cross section from gluon fusion processes. By a detailed numerical analysis using the open-source platform `xFitter`, we find that high-statistics determinations of the longitudinally polarized angular coefficient at the LHC Run III and high-luminosity HL-LHC improve the PDF systematic uncertainties of the Higgs boson cross section predictions by 50% over a broad range of Higgs boson rapidities.

Introduction

Precision studies in the Higgs sector of the Standard Model (SM) are central to current [1] and forthcoming [2] physics programs at the Large Hadron Collider (LHC), and provide a portal to searches for beyond-Standard-Model (BSM) physics. The dominant mechanism for the production of Higgs bosons in proton-proton collisions at the LHC is given by the fusion of two gluons resolved from the incoming protons. With the very high accuracy reached in perturbative Quantum Chromodynamics (QCD) calculations of gluon-initiated production cross sections, currently of next-to-next-to-next-to-leading order (N^{3}LO) [3–5] in the QCD coupling α_s, the theoretical systematic uncertainties affecting the predictions for gluon fusion processes receives essential contributions from the non-perturbative gluon parton density function (PDF), as well as the sea-quark densities coupled to gluons through initial-state QCD evolution. See e.g. [2], where the PDF contribution is estimated to be about 30 % of the total uncertainty, including α_s and scale variations.

The primary source of knowledge of the gluon PDF is given at present, in global fits to hadron collider data [6–12], by deep inelastic scattering (DIS) experimental measurements at high energy. Future DIS experiments [13,14] are proposed to extend the range and accuracy of our current knowledge of the gluon PDF. It is hoped that substantial progress can also come from measurements at the LHC itself, particularly in the forthcoming high-luminosity phase HL-LHC [15]. Gluon PDF determinations are considered from open [16,17] and bound-state [18] charm and bottom quark production, light-quark jets [19] and top quark production [20].

In this work we take color-singlet hadro-production (unlike the above cases, in which the Born-approximation final state contains colored particles) and, similarly to the case of DIS, investigate the sensitivity to the gluon PDF via $\mathcal{O}(\alpha_s)$ contributions, guided by criteria of perturbative stability and experimental precision.

We consider Drell-Yan (DY) charged lepton-pair production [21] via electroweak vector boson exchange. Let us map the DY cross section in the boson invariant mass M, rapidity Y and transverse

* Corresponding author.
E-mail addresses: simone.amoroso@desy.de (S. Amoroso), fiaschi@uni-muenster.de (J. Fiaschi), francesco.giuli@roma2.infn.it (F. Giuli), alexander.glazov@desy.de (A. Glazov), hautmann@thphys.ox.ac.uk (F. Hautmann), oleksandr.zenaiev@cern.ch (O. Zenaiev).

https://doi.org/10.1016/j.physletb.2021.136613

momentum p_T, and in the lepton polar and azimuthal angles θ and ϕ, defined in the Collins-Soper reference frame [22] (see e.g. the DY cross section parameterization in [23]). The DY cross section summed over the electroweak boson polarizations has the angular distribution $1+\cos^2\theta$ and is sensitive to the gluon PDF for finite p_T. However, in the p_T region where the cross section is the largest, it is affected by large perturbative corrections to all orders in α_s (see e.g. [24], and references therein). Let us turn to contributions of the single electroweak-boson polarizations. The diagonal elements of the polarization density matrix [22,25–27] in the helicity basis yield (besides the unpolarized cross section, proportional to the trace of the density matrix) the forward-backward asymmetry and the longitudinally polarized cross section, associated respectively with angular distributions $\cos\theta$ and $(3\cos^2\theta-1)/2$. The former is parity-violating and dominated by flavor non-singlet PDFs [28–34]. The latter is parity-conserving and sensitive to flavor singlet PDFs. Off-diagonal density matrix elements can be accessed by measuring, besides θ, the lepton's azimuthal angle ϕ, and yield six additional contributions besides the previous three, leading to nine linearly independent polarized cross sections, which correspond to the first nine terms in the expansion over spherical harmonics.

In order to constrain the Higgs boson production cross section from gluon fusion, we will focus on the ratio of the longitudinal electroweak boson cross section to the unpolarized cross section, defining the angular coefficient

$$A_0(s,M,Y,p_T)=\frac{2d\sigma^{(L)}/dMdYdp_T}{d\sigma/dMdYdp_T}. \qquad (1)$$

The coefficient A_0 is perturbatively stable, as illustrated by the smallness of its next-to-leading-order (NLO) [35–40] and next-to-next-to-leading-order (NNLO) [41] radiative corrections for finite p_T, and precisely measured at the LHC [23,42], following earlier measurements at the Tevatron [43] and fixed-target experiments [44–48]. We will comment later on the extension of the analysis to other polarized contributions besides the longitudinal cross section.

We now proceed as follows. First, we discuss the general properties of the angular coefficient (1) illustrating the physics potential of precision measurements of DY angular distributions at the LHC Run III and HL-LHC. Next, we focus on its application to the profiling of the gluon distribution using the open-source fit platform `xFitter` [49], and compute the resulting Higgs boson cross section and PDF uncertainty at $\sqrt{s}=13$ TeV.

Longitudinally polarized angular coefficient

The longitudinally polarized coefficient A_0 in Eq. (1) vanishes in the parton model and receives leading-order (LO) perturbative QCD contributions at $\mathcal{O}(\alpha_s)$. We evaluate A_0 at LO and NLO (i.e., through $\mathcal{O}(\alpha_s^2)$) using the `MadGraph5_aMC@NLO` [50] program for Z + 1 parton pp production. In Fig. 1[1] we show results for A_0 at the energy $\sqrt{s}=13$ TeV versus the boson p_T for three distinct kinematic regions: two of them at central rapidity $|Y|<1$ with invariant mass M close to the Z boson mass M_Z as well as between the J/ψ and Υ resonances, corresponding to ATLAS and CMS kinematics; and one with $2<|Y|<4.5$ and M close to M_Z, corresponding to LHCb kinematics. We also show separately the contributions to A_0 from the initial-state partonic channels $q\bar{q}$ and qg (qq and gg channels are present at NLO, but they are suppressed by relative order α_s).

[1] While no cut is applied on the parton p_T, a cut on the Z-boson p_T of 11.4 GeV is used for calculations in the Z-boson mass region. This is lowered to 1 GeV for the low-mass region.

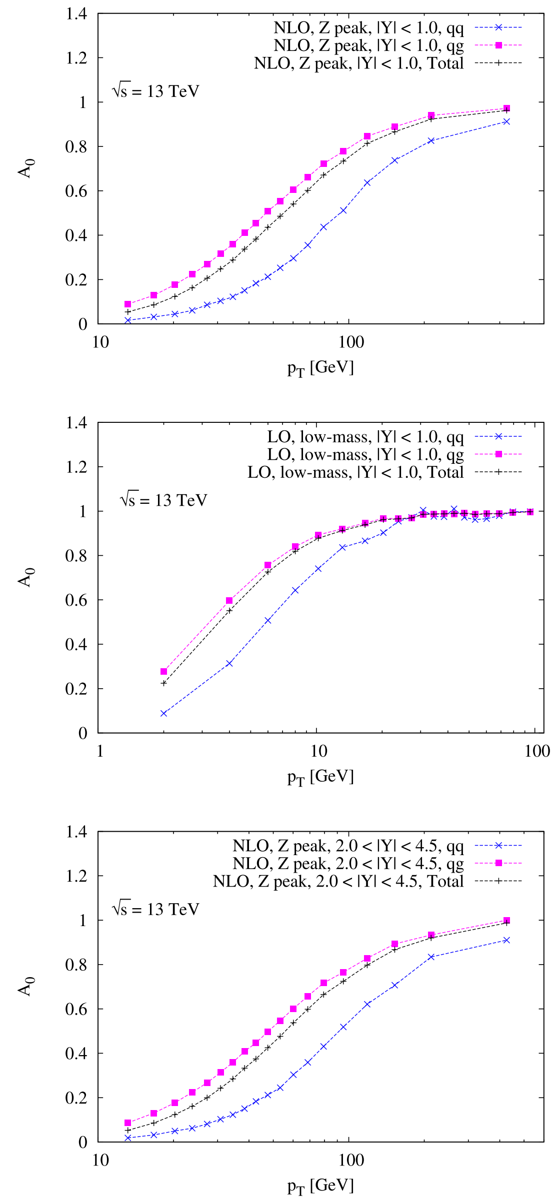

Fig. 1. The angular coefficient A_0 and its $q\bar{q}$, qg contributions for $\sqrt{s}=13$ TeV as functions of the boson p_T based on CT18nnlo PDF set. The results are plotted in different regions of the boson invariant mass M and rapidity Y: the Z-boson peak region, 80 GeV $<M<$ 100 GeV, for $|Y|<1.0$ (NLO, top); low-mass region between the J/Ψ and Υ resonances, 4 GeV $<M<$ 8 GeV, for $|Y|<1.0$ (LO, center); Z-boson peak region, 80 GeV $<M<$ 100 GeV for LHCb kinematics (NLO, bottom).

The coefficient A_0 as well as its $q\bar{q}$ and qg components rise monotonically from 0 at $p_T=0$ to 1 for $p_T\gg M$. The gluonic channel qg dominates over the fermionic channel $q\bar{q}$, for the low mass region in particular. The weight of the $q\bar{q}$ contribution increases for the Z pole region and reaches its largest value for the LHCb phase space. This can be understood since the range in longitudinal momentum fraction x probed for the PDFs is changing from low to high x. The location of A_0 measured in experimental data with respect to the predicted $q\bar{q}$ and qg contributions can constrain the $\bar{q}/g$ ratio.

The main sensitivity to the gluon distribution arises from the A_0 region with the largest slope in p_T, i.e., around the turn-over point $\partial^2 A_0/\partial p_T^2=0$. Fig. 1 illustrates that the position of this turn-over point varies strongly with a power-like dependence on the lepton-pair invariant mass, so that the mass provides a powerful handle on the p_T scales probed in the initial state distribution.

Near the Z-boson peak the turn-over occurs at p_T of the order of several ten to 100 GeV, while at low masses, between the J/Ψ and Υ meson resonances, it is at p_T of the order of a few GeV. This behavior is to be contrasted with the case of $d\sigma/dp_T$, which peaks at low p_T, with the position of the peak depending only very mildly on the invariant mass [22,24]. Thus, we will use the longitudinally polarized angular distribution near the electroweak boson mass scale in order to constrain the gluon PDF in the region relevant [51] for Higgs boson production (as will be described next). On the other hand, the above observations on the meson resonance region suggest that the angular distribution in this region can provide sensitivity to the p_T dependent PDFs [24,52–54] (which we leave to future investigations).

New features therefore arise in the extraction of non-perturbative QCD contributions owing to the vector boson polarization. In what follows, we carry out a detailed analysis for collinear distributions.

Gluon profiling and Higgs cross section

To analyze the impact of high-precision A_0 measurements on the Higgs boson production cross section, we implement the NLO `MadGraph5_aMC@NLO` A_0 calculation into the fit platform `xFitter` [49]. First, we validate our implementation by performing NLO fits to the $\sqrt{s} = 8$ TeV ATLAS measurements [23] of A_0, and verifying that good χ^2 values are obtained for all the PDF sets considered, namely CT18nnlo [6], NNPDF3.1nnlo [7], ABMP16nnlo [8], HERAPDF2.0nnlo [11] and MSHT20nnlo [12]. Next, we generate A_0 pseudodata for Z $p_T > 11.4$ GeV at $\sqrt{s} =$ 13 TeV for two projected luminosity scenarios of 300 fb^{-1} (the designed integrated luminosity at the end of the LHC Run III) and 3 ab^{-1} (the designed integrated luminosity at the end of the HL-LHC stage [15]), and apply the profiling technique [55,56] to evaluate the PDF uncertainties. To do this, we extrapolate the statistical uncertainties for the two projected integrated luminosities, and estimate the systematic uncertainties assuming a 0.1% systematic uncertainties in the lepton momentum scale.[2] We perform the analysis in the mass region 80 GeV $< M <$ 100 GeV around the Z-boson peak and rapidity region $|Y| < 3.5$. The results are reported in Fig. 2.

We find that, in accord with the earlier discussion, the largest reduction of uncertainties from the high-luminosity A_0 profiling occurs for the gluon density (top two panels in Fig. 2), and for the u and d sea-quark densities coupled to gluons through QCD evolution (bottom two panels in Fig. 2). All panels in Fig. 2 show the range $10^{-3} \lesssim x \lesssim 10^{-1}$ where the reduction is most pronounced. We find that the largest sensitivity comes from transverse momenta in the mid range $p_T \sim 50$ GeV, and the sensitivity dies out for $p_T \gtrsim 100$ GeV. The current-to-300 fb^{-1} gain dominates the 300 fb^{-1} to 3 ab^{-1} gain, similarly to other earlier profiling examples (see detailed discussions in [28] for valence quarks and in [57] for gluons).

We have also verified the perturbative stability of our results, by repeating the profiling with a variation of the perturbative factorization and renormalization scales at NLO in the pseudodata. The central value for the resulting gluon distribution function stays within one standard deviation band of the profiled PDF uncertainty. Given that existing NNLO predictions have significantly reduced scale uncertainty [41], we expect that the effect of higher-order corrections will have only a small impact on the profiled PDFs, and this uncertainty is neglected in the following.

[2] Note that PDF uncertainties are large in the ATLAS 8 TeV A_0 measurements [23] extrapolated in rapidity Y, but they are small for the measurements [23] in bins of Y.

The effect of the longitudinally polarized coefficient on the $Q^2 = 10^4$ GeV^2 gluon PDF near $x \sim 10^{-2}$ will influence the Higgs boson cross section. To study this, we compute SM Higgs boson production in the gluon fusion mode for $\sqrt{s} = 13$ TeV pp collisions, using the MCFM code [58,59] at NLO in QCD perturbation theory. We evaluate PDF uncertainties on the Higgs cross section including constraints from A_0 profiling. The results are given in Fig. 3 versus the Higgs boson rapidity y_H. We see that in the region $-2 \lesssim y_H \lesssim 2$ the uncertainty is reduced by about 30–40% in the Run III scenario, and a further reduction to about 50% takes place in the HL-LHC scenario.

We next perform a higher-order N^{3}LO calculation for the Higgs boson total cross section using the code `ggHiggs` [60,61]. In Fig. 4, we report the result for the cross section and its uncertainty in the cases of the current CT18nnlo [6], NNPDF3.1nnlo [7] and MSHT20nnlo [12] global sets as well as projected sets, based on complete LHC data sample [62]. The PDF4LHC15scen1/2 sets, which are PDF projections including HL-LHC pseudodata, also show a smaller, but not negligible, reduction in uncertainties. Notwithstanding the numerical differences, the behavior is qualitatively similar for the different sets, and provides further support at N^{3}LO to the picture given in Fig. 3 for the NLO Higgs boson rapidity cross section.

The results above for the Higgs boson production cross section have been obtained using the DY angular coefficient for longitudinal electroweak boson polarization in the mass region near the Z-boson mass (top panel in Fig. 1). We stress that the same approach, extended to mass regions away from the Z peak, has the potential to provide complementary physics information. For instance, high-mass DY angular distributions allow the region of larger x momentum fractions to be accessed and will be relevant for associated Higgs boson production with a gauge/Higgs boson or heavy-flavor quarks. Conversely, we have noted earlier that measurements of A_0 at low masses (center panel in Fig. 1) may be used to probe p_T dependent gluon PDF effects, and this will impact the Higgs boson p_T spectrum for low transverse momenta. The extension to low masses can further provide a handle on the small-x regime [61,63] of Higgs boson production relevant to the highest energy frontier.

We have so far exploited the sensitivity of the longitudinal electroweak boson polarization to the gluon PDF and singled out A_0 as a perturbatively stable observable, which can be built via diagonal elements of the polarization density matrix and is measurable via the lepton polar angle θ. This can be generalized as further sensitivity may arise from off-diagonal density matrix elements via longitudinal-transverse interferences, such as the parity-conserving A_1 and parity-violating A_3 coefficients [23], which can be accessed by measuring also the lepton azimuthal angle ϕ. These coefficients are generally smaller than A_0 and with a milder p_T dependence, but provide a more pronounced Y rapidity dependence. Moreover, starting at order α_s^2 one may investigate additional handles from violation of the Lam-Tung relation [25], $A_2 \neq A_0$, and from the T-odd coefficients A_5, A_6, A_7 [23].

Conclusion

We have proposed the systematic use of electroweak gauge boson polarization in charged lepton-pair hadro-production to investigate gluon-initiated processes and the associated non-perturbative QCD contributions.

We have illustrated this by studying the implications of precise measurements of the angular coefficient A_0 near the Z-boson mass scale on the theoretical predictions for the Higgs boson production cross section, exploiting the coupling of the longitudinal polarization to the gluon PDF through radiative contributions in α_s.

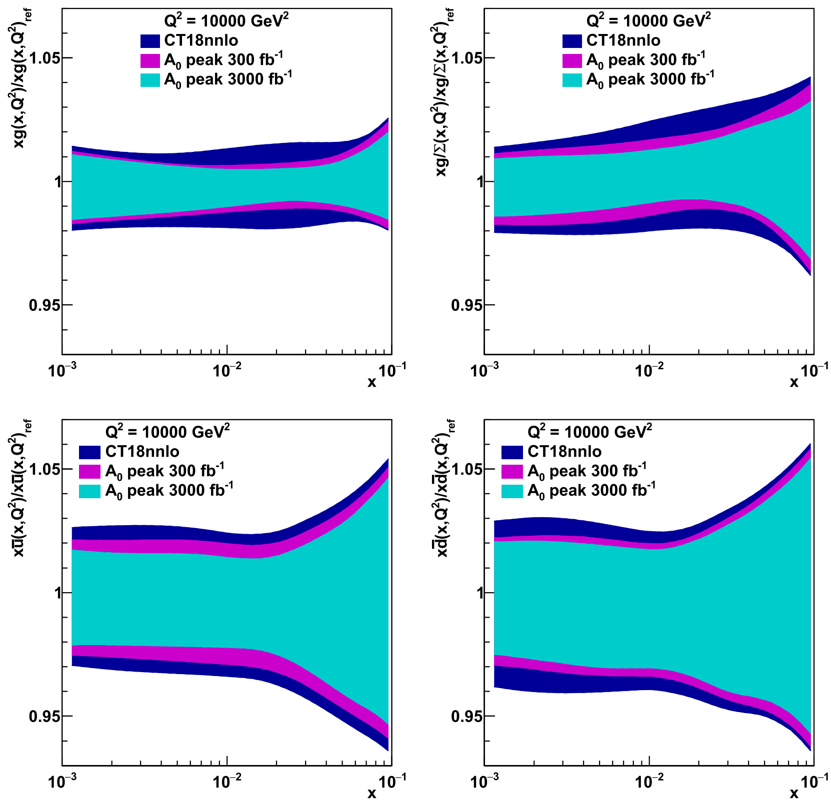

Fig. 2. Original CT18nnlo [6] (red) and profiled distributions using A_0 pseudodata corresponding to integrated luminosities of 300 fb^{-1} (blue) and 3 ab^{-1} (green) for 80 GeV $< M <$ 100 GeV and $|Y| < 3.5$. Results for gluon (xg), gluon/Sea (xg/Σ), u-type ($x\bar{u}$) and d-type ($x\bar{d}$) sea-quark densities are shown for $Q^2 = 10^4$ GeV^2. Bands represent PDF uncertainties, shown at the 68% CL.

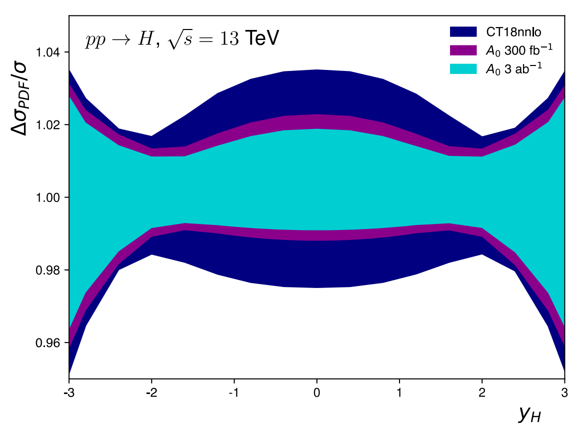

Fig. 3. Ratio of PDF uncertainties for the gluon-gluon fusion SM Higgs boson cross-section in pp collisions at $\sqrt{s}=13$ TeV as a function of the Higgs rapidity. The red band shows the uncertainties of the CT18nnlo PDF set [6], reduced to 68% CL coverage. The blue and green bands show the uncertainties of the CT18nnlo including constraints from the A_0 measurement and assuming 300 fb^{-1} and 3 ab^{-1}, respectively.

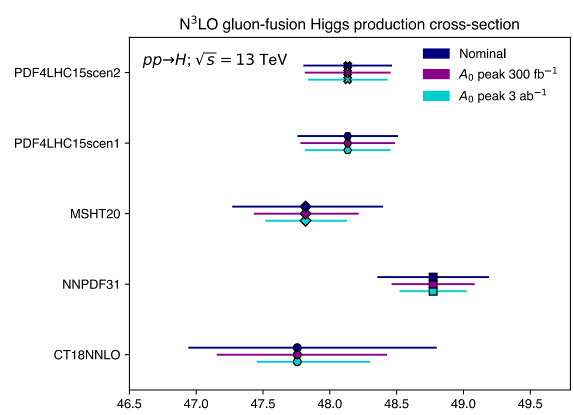

Fig. 4. The gluon-gluon fusion Higgs boson production cross-section at N^{3}LO for different PDFs, showing the uncertainty from PDFs and their expected reduction including constraints from the A_0 measurement assuming 300 fb^{-1} and 3 ab^{-1}, respectively.

Our results open a new area of phenomenological studies on connections between the gauge and Higgs sectors of the SM, as further aspects may be investigated via generalization to the full structure of lepton angular distributions, including polarization interferences, and to mass regions far away from the Z-boson peak.

Declaration of competing interest

The authors declare that they have no known competing financial interests or personal relationships that could have appeared to influence the work reported in this paper.

Acknowledgements

We thank H. Abdolmaleki, A. Armbruster, V. Bertone, S. Camarda, A. Cooper-Sarkar, D. Britzger, L. Harland-Lang, A. Huss, F. Olness and other `xFitter` developers for useful conversations and advice. The work of JF has been supported by the BMBF under contract 05H15PMCCA and the DFG through the Research Training Network 2149 “Strong and weak interactions - from hadrons to dark matter” and by STFC under the consolidated grant ST/T000988/1.

Appendix A. Supplementary material

Supplementary material related to this article can be found online at https://doi.org/10.1016/j.physletb.2021.136613.

References

[1] D. de Florian, et al., LHC Higgs Cross Section Working Group, arXiv:1610.07922 [hep-ph].
[2] M. Cepeda, et al., CERN Yellow Rep. Monogr., vol. 7, 2019, p. 221, arXiv:1902.00134 [hep-ph].
[3] X. Chen, T. Gehrmann, E.W.N. Glover, A. Huss, B. Mistlberger, A. Pelloni, Phys. Rev. Lett. 127 (2021) 072002, arXiv:2102.07607 [hep-ph].
[4] F. Dulat, B. Mistlberger, A. Pelloni, Phys. Rev. D 99 (2019) 034004, arXiv:1810.09462 [hep-ph].
[5] C. Anastasiou, et al., J. High Energy Phys. 05 (2016) 058, arXiv:1602.00695 [hep-ph].
[6] T.J. Hou, J. Gao, T.J. Hobbs, K. Xie, S. Dulat, M. Guzzi, J. Huston, P. Nadolsky, J. Pumplin, C. Schmidt, et al., Phys. Rev. D 103 (2021) 014013, arXiv:1912.10053 [hep-ph].
[7] R.D. Ball, et al., NNPDF Collaboration, Eur. Phys. J. C 77 (2017) 663, arXiv:1706.00428 [hep-ph].
[8] S. Alekhin, et al., Phys. Rev. D 96 (2017) 014011, arXiv:1701.05838 [hep-ph].
[9] L. Harland-Lang, et al., Eur. Phys. J. C 75 (2015) 204, arXiv:1412.3989 [hep-ph].
[10] R.D. Ball, et al., NNPDF Collaboration, J. High Energy Phys. 1504 (2015) 040, arXiv:1410.8849 [hep-ph].
[11] H. Abramowicz, et al., H1 ZEUS, Eur. Phys. J. C 75 (2015) 580, arXiv:1506.06042 [hep-ex].
[12] S. Bailey, T. Cridge, L.A. Harland-Lang, A.D. Martin, R.S. Thorne, Eur. Phys. J. C 81 (2021) 341, arXiv:2012.04684 [hep-ph].
[13] P. Agostini, et al., LHeC and FCC-he Study Group, arXiv:2007.14491 [hep-ex].
[14] C. Aidala, et al., arXiv:2002.12333 [hep-ph].
[15] P. Azzi, et al., CERN Yellow Rep. Monogr., vol. 7, 2019, p. 1, arXiv:1902.04070 [hep-ph].
[16] O. Zenaiev, et al., PROSA, J. High Energy Phys. 04 (2020) 118, arXiv:1911.13164 [hep-ph].
[17] M. Cacciari, M.L. Mangano, P. Nason, Eur. Phys. J. C 75 (2015) 610, arXiv:1507.06197 [hep-ph].
[18] C.A. Flett, et al., Phys. Rev. D 101 (2020) 094011, arXiv:1908.08398 [hep-ph].
[19] R. Abdul-Khalek, et al., Eur. Phys. J. C 80 (2020) 797, arXiv:2005.11327 [hep-ph].
[20] M. Czakon, et al., J. High Energy Phys. 04 (2017) 044, arXiv:1611.08609 [hep-ph].
[21] S. Drell, T.-M. Yan, Phys. Rev. Lett. 25 (1970) 316.
[22] J.C. Collins, D.E. Soper, Phys. Rev. D 16 (1977) 2219.
[23] G. Aad, et al., ATLAS, J. High Energy Phys. 08 (2016) 159, arXiv:1606.00689 [hep-ex].
[24] R. Angeles-Martinez, et al., Acta Phys. Pol. B 46 (2015) 2501, arXiv:1507.05267 [hep-ph].
[25] C.S. Lam, W.K. Tung, Phys. Rev. D 18 (1978) 2447.
[26] M. Chaichian, M. Hayashi, K. Yamagishi, Phys. Rev. D 25 (1982) 130, erratum: Phys. Rev. D 26 (1982) 2534.
[27] K. Hagiwara, K. Hikasa, N. Kai, Phys. Rev. Lett. 52 (1984) 1076.
[28] E. Accomando, et al., J. High Energy Phys. 1910 (2019) 176, arXiv:1907.07727 [hep-ph].
[29] H. Abdolmaleki, et al., arXiv:1907.08301 [hep-ph].
[30] E. Accomando, et al., Eur. Phys. J. C 78 (2018) 663, arXiv:1805.09239 [hep-ph].
[31] E. Accomando, et al., Phys. Rev. D 98 (2018) 013003, arXiv:1712.06318 [hep-ph].
[32] J. Fiaschi, et al., PoS DIS 2019 (2019) 012, arXiv:1906.11793 [hep-ph].
[33] E. Accomando, et al., Phys. Lett. B 803 (2020) 135293, arXiv:1910.13759 [hep-ph].
[34] J. Fiaschi, et al., arXiv:1805.00842 [hep-ph].
[35] E. Mirkes, Nucl. Phys. B 387 (1992) 3.
[36] E. Mirkes, J. Ohnemus, Phys. Rev. D 50 (1994) 5692, arXiv:hep-ph/9406381 [hep-ph].
[37] E. Mirkes, J. Ohnemus, Phys. Rev. D 51 (1995) 4891, arXiv:hep-ph/9412289 [hep-ph].
[38] M. Lambertsen, W. Vogelsang, Phys. Rev. D 93 (2016) 114013, arXiv:1605.02625 [hep-ph].
[39] J.C. Peng, et al., Phys. Lett. B 758 (2016) 384, arXiv:1511.08932 [hep-ph].
[40] W.C. Chang, et al., Phys. Rev. D 96 (2017) 054020, arXiv:1708.05807 [hep-ph].
[41] R. Gauld, et al., J. High Energy Phys. 11 (2017) 003, arXiv:1708.00008 [hep-ph].
[42] V. Khachatryan, et al., CMS, Phys. Lett. B 750 (2015) 154, arXiv:1504.03512 [hep-ex].
[43] T. Aaltonen, et al., CDF, Phys. Rev. Lett. 106 (2011) 241801, arXiv:1103.5699 [hep-ex].
[44] S. Falciano, et al., NA10, Z. Phys. C 31 (1986) 513.
[45] M. Guanziroli, et al., NA10, Z. Phys. C 37 (1988) 545.
[46] J.S. Conway, et al., E615, Phys. Rev. D 39 (1989) 92.
[47] L.Y. Zhu, et al., NuSea, Phys. Rev. Lett. 99 (2007) 082301, arXiv:hep-ex/0609005 [hep-ex].
[48] L.Y. Zhu, et al., NuSea, Phys. Rev. Lett. 102 (2009) 182001, arXiv:0811.4589 [nucl-ex].
[49] S. Alekhin, et al., Eur. Phys. J. C 75 (2015) 304, arXiv:1410.4412 [hep-ph].
[50] J. Alwall, et al., J. High Energy Phys. 07 (2014) 079, arXiv:1405.0301 [hep-ph].
[51] P. Cipriano, et al., Phys. Rev. D 88 (2013) 097501, arXiv:1308.1655 [hep-ph].
[52] L. Motyka, M. Sadzikowski, T. Stebel, Phys. Rev. D 95 (2017) 114025, arXiv:1609.04300 [hep-ph].
[53] D. Boer, et al., SciPost Phys. 3 (2017) 040, arXiv:1709.04935 [hep-ph].
[54] F. Hautmann, I. Scimemi, A. Vladimirov, Phys. Lett. B 806 (2020) 135478, arXiv:2002.12810 [hep-ph].
[55] H. Paukkunen, P. Zurita, J. High Energy Phys. 1412 (2014) 100, arXiv:1402.6623 [hep-ph].
[56] S. Camarda, et al., Eur. Phys. J. C 75 (2015) 458, arXiv:1503.05221 [hep-ph].
[57] J. Rojo, et al., J. Phys. G 42 (2015) 103103, arXiv:1507.00556 [hep-ph].
[58] J.M. Campbell, R.K. Ellis, Nucl. Phys. B, Proc. Suppl. 205–206 (2010) 10, arXiv:1007.3492 [hep-ph].
[59] J. Campbell, T. Neumann, J. High Energy Phys. 12 (2019) 034, arXiv:1909.09117 [hep-ph].
[60] M. Bonvini, et al., J. Phys. G 41 (2014) 095002, arXiv:1404.3204 [hep-ph].
[61] M. Bonvini, S. Marzani, Phys. Rev. Lett. 120 (2018) 202003, arXiv:1802.07758 [hep-ph].
[62] R. Abdul-Khalek, et al., Eur. Phys. J. C 78 (2018) 962, arXiv:1810.03639 [hep-ph].
[63] F. Hautmann, Phys. Lett. B 535 (2002) 159, arXiv:hep-ph/0203140 [hep-ph].